

Scaling investigation for the dynamics of charged particles in an electric field accelerator

Denis Gouvêa Ladeira and Edson D. Leonel

Citation: *Chaos* **22**, 043148 (2012); doi: 10.1063/1.4772997

View online: <http://dx.doi.org/10.1063/1.4772997>

View Table of Contents: <http://chaos.aip.org/resource/1/CHAOEH/v22/i4>

Published by the AIP Publishing LLC.

Additional information on Chaos

Journal Homepage: <http://chaos.aip.org/>

Journal Information: http://chaos.aip.org/about/about_the_journal

Top downloads: http://chaos.aip.org/features/most_downloaded

Information for Authors: <http://chaos.aip.org/authors>

ADVERTISEMENT



Scaling investigation for the dynamics of charged particles in an electric field accelerator

Denis Gouvêa Ladeira¹ and Edson D. Leonel^{2,3}

¹*Departamento de Física e Matemática, Univ. Federal de São João del-Rei, UFSJ, Rod. MG 443, Km 7, Fazenda do Cadete, 36420-000 Ouro Branco, MG, Brazil*

²*Departamento de Física, Univ. Estadual Paulista, UNESP, Av. 24A, 1515, Bela Vista, 13506-900 Rio Claro, SP, Brazil*

³*Abdus Salam ICTP, 34100 Trieste, Italy*

(Received 12 June 2012; accepted 5 December 2012; published online 28 December 2012)

Some dynamical properties of an ensemble of trajectories of individual (non-interacting) classical particles of mass m and charge q interacting with a time-dependent electric field and suffering the action of a constant magnetic field are studied. Depending on both the amplitude of oscillation of the electric field and the intensity of the magnetic field, the phase space of the model can either exhibit: (i) regular behavior or (ii) a mixed structure, with periodic islands of regular motion, chaotic seas characterized by positive Lyapunov exponents, and invariant Kolmogorov–Arnold–Moser curves preventing the particle to reach unbounded energy. We define an escape window in the chaotic sea and study the transport properties for chaotic orbits along the phase space by the use of scaling formalism. Our results show that the escape distribution and the survival probability obey homogeneous functions characterized by critical exponents and present universal behavior under appropriate scaling transformations. We show the survival probability decays exponentially for small iterations changing to a slower power law decay for large time, therefore, characterizing clearly the effects of stickiness of the islands and invariant tori. For the range of parameters used, our results show that the crossover from fast to slow decay obeys a power law and the behavior of survival orbits is scaling invariant. © 2012 American Institute of Physics. [<http://dx.doi.org/10.1063/1.4772997>]

The formalism of escape is used to study the dynamics and hence the transport of charged particles in an accelerator. The model consists of a periodically time dependent electric field limited to a certain region in space that furnishes or absorbs energy of a particle. After the particle leaves the electric field region, a constant magnetic field impels the particle to move in a circular trajectory. This magnetic field is responsible for bringing the particle back to the electric field region leaving the energy unchanged. The control parameters ε and τ represent the amplitude of the time-dependent electric field and the inverse of the magnetic field, respectively. The parameter ε defines the nonlinear strength while $\pi\tau$ defines the time that the particle spends in the magnetic region. The dynamics can be described by a two-dimensional nonlinear mapping. Depending on both ε and τ , the phase space presents either regular or mixed structure. For $\varepsilon = 0$, the nonlinear term vanishes and the particle's energy is constant in time. For $\tau = 1, 3, 5, \dots$, there is a strong correlation between the frequency of oscillation of the electric field and the intensity of the magnetic field, and as a consequence, the motion of the particle is regular. For different control parameters than those discussed, the phase space presents mixed structure with islands of regular motion surrounded by chaotic seas and invariant KAM curves that prevent the particle from acquiring unbounded energy gain. We study the escape of particles through a hole in the phase space placed in the velocity axis by considering the position of the lowest energy KAM curve. An ensemble of trajectories evolves in time from low energy until each reaches the escaping hole or a

maximum time. This formalism is used to study the transport of particles through the chaotic region of the phase space. We obtain both the histogram of exit times as well as the survival probability as functions of n (number of egresses from the region of the electric field). The survival probability decays exponentially for short n and, due to the existence of sticky domains, it decays as a power law for large n . Both the histogram of escape and the survival probability are described using scaling approach.

I. INTRODUCTION

As an attempt to explain the origin of high energy cosmic rays, Fermi proposed a simple model¹ where charged particles interact with time dependent magnetic fields. Such interaction triggered a mechanism leading them to exhibit an enormous energy growth. The phenomena of unlimited energy gain, also known as Fermi acceleration (FA), is a subject of interest since the observation of such high energy particles and therefore applications of FA are observed in different fields of science including plasma physics,² astrophysics,^{3,4} atomic physics,⁵ optics,^{6,7} and even in the well known time dependent billiard problems.⁸

The model proposed by Fermi was latter modified to simulate other systems, under different applications and approaches. One of them^{9,10} assumes that the dynamics is given by a classical particle (to denote the cosmic ray) confined to bounce inside two rigid walls: one of them is

periodic in time (simulating the time varying magnetic fields) and the other is fixed (working as a returning mechanism of the particle for a next collision). This version of the model is known as Fermi-Ulam model (FUM). The dynamics depends on a single control parameter which relates to the relative amplitude of motion of the moving wall. For non null control parameter, the structure of the phase space is mixed leading to the observation of periodic islands surrounded by a chaotic sea and invariant KAM curves (also known in the literature as rotational invariant circle or invariant spanning curve) which prevent the particle to accumulate unbounded energy. For zero amplitude of motion of the oscillating wall, the system is integrable.

Another version of the Fermi model consists of a classical particle that falls freely in a constant gravitation field and collides with a periodically moving platform. In this model, the returning mechanism is due to the gravitation field and it is called *bouncer* or Fermi-Pustilnikov model (FPM).¹¹ The FPM can also be described in terms of dimensionless variables leading to a single control parameter that controls two types of transition: (i) integrability to non-integrability and (ii) limited to unlimited energy growth.¹²

Latter on, a hybrid version of the two models was proposed¹³ and it presents properties of both models. In particular, properties of the FUM are recovered on the limit of vanishing gravitational field and properties of the FPM are observed in the limit of strong gravitation field. There is, however, a range of control parameters where the Lyapunov exponent passes by a maximum and it was interpreted as being a competition between the two models to dominate over the dynamics of the particle. A dissipative version of this hybrid model was also discussed¹⁴ leading to the observation of boundary crisis and annihilation of fixed points.

In this paper, we study a type of Fermi accelerator model that neither is a FUM, nor is a FPM. The model under study is a modification of the so called *cyclotron* accelerator. We have to emphasize however that the energies and velocities we are considering in this paper are far from the relativistic domain. It is known in the literature however that the cyclotron with an infinitesimal gap can be modeled exactly by the Standard map (for specific discussions see Ref. 15 and references therein). Indeed, cyclotrons find applications in medicine, where production of therapeutic quantities of Auger emitter from several different isotopes is important in targeted radionuclide therapy of small tumors.^{16,17} Modern cyclotrons developments are concerned to the production of the standard isotopes and also new therapeutic isotopes.¹⁸ Applications of cyclotron accelerators include also technological processes, as ion beam lithography.^{19,20}

The model under study here consists in the motion of a classical particle with charge q and mass m that interacts with a time dependent electric field in the presence of a constant magnetic field. The electric field oscillates with amplitude E_0 and the magnetic field H is assumed to be uniform. For null amplitude of oscillation of electric field, the energy of the particle is constant. For $E_0 \neq 0$, the system becomes non-integrable. With exception of specific values of H , the phase space of the system presents a remarkably intricate mixed structure for $E_0 \neq 0$. We observe periodic islands

surrounded by chaotic seas characterized by positive values of Lyapunov exponent, and invariant KAM curves limiting the energy gain of the particle. As we discuss ahead, this model has a different re-injection mechanism as compared to the FUM and FPM, leading therefore to interesting properties and scaling, that for the knowledge of the authors, were not yet discussed in the literature. Our main goal on this model is to understand and describe some scaling properties of the chaotic sea, focusing specifically in the transport properties.

We define an escape velocity in the chaotic sea as a fraction of the velocity in the lowest energy invariant KAM curve. Then we define an escape window as the region of phase space between the escape velocity and this KAM curve. Starting with very low energy, we let an ensemble of particles to evolve along the phase space. Each initial condition (particle) is evolved individually until the entire ensemble is considered. When the particles achieve the critical velocity we stop the orbits (that would be equivalent to the escape) and calculate average observables. It is known that, for fully chaotic dynamics, the survival probability for the orbits which last longer in the dynamics until escape through the escape window presents an exponential decay.²¹ For mixed structures, however, the stickiness responsible for trapping particles near periodic islands and invariant tori produces a slower decay which may be a power law type²² or stretched exponential.²³

This paper is organized as follows. In Sec. II, we present the details of the model and obtain the two-dimensional mapping that describes the dynamics of the particle. Then we use Lyapunov exponents and show that the system presents a chaotic sea for different combinations of values of control parameters. We reserve the scaling discussion for Sec. III, where we obtain the critical exponents and overlaps of the escape distribution and surviving probability curves. We present final discussions and remarks in Sec. IV.

II. THE MODEL AND PHASE SPACE PROPERTIES

The model under consideration consists of a classical particle of mass m and electrical charge q that interacts with a time-dependent electric field denoted by $\vec{E}(t')$, where t' is the variable time. Moreover, the particle suffers the action of a constant magnetic field $\vec{H} = H\hat{z}$, where \hat{z} is a unity vector that points at increasing z direction. We assume the electric field varies according to $\vec{E}(t') = E_0 \cos(\omega t' + \phi_0) \hat{x}$ and it acts only in the region between $x = 0$ and $x = d$. The quantity E_0 denotes the amplitude, ω is the frequency, ϕ_0 is the initial phase of oscillation of the electric field, and \hat{x} corresponds to the unity vector pointing at increasing x direction. By definition, $\vec{E}(t')$ and \vec{H} are orthogonal vectors. This system can be thought as a modification of the cyclotron accelerator, where the frequency ω of $\vec{E}(t')$ is not necessarily the cyclotron frequency, namely $\varpi = qH/m$. We stress however the energies and velocity we are considering in this paper are low enough so that the model is not in the relativistic domain. The vertical lines in Fig. 1 represent the boundaries of the region where the time dependent electric field, which is generated by a pair of electrodes, is confined. Depending on the

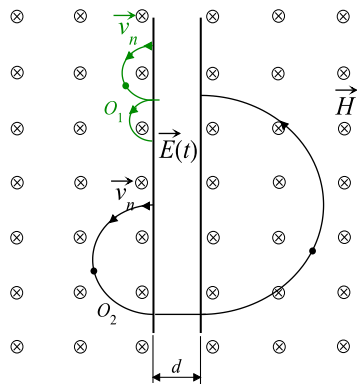


FIG. 1. Pieces of two possible orbits in the proposed model. The upper trajectory illustrates a situation where the particle enters into and leaves from the electric field region at $x=0$. The lower trajectory illustrates a situation where the particle enters into the electric field at the left side and leaves this region at $x=d$.

velocity and control parameters, the particle can: (i) enter in and leave from the electric field region at the same side or; (ii) enter in from a side and leave out from the other side. Figure 1 illustrates pieces of two possible trajectories.

During the time that the particle is immerse in the region where electric field acts, a force $\vec{F}(t') = q\vec{E}(t')$ accelerates the particle. Depending on the velocity of the particle and phase of oscillation of the electric field, the particle can gain or lose energy from the field. Regarding \hat{y} is perpendicular to \hat{x} , if the initial velocity of particle includes a component parallel to \hat{y} , $v_{y,0}$, this component is not affected by the electric force. In this case $v_y = v_{y,0}$, all the times the particle leaves the field $\vec{E}(t')$. Therefore, we consider the situation where $v_{y,0} = 0$. From the second Newton's law, we obtain the following expression for the position of the particle in the electric field region

$$x(t') = x_i + \left[v_i - \frac{E_0 q}{\omega m} \sin(\omega t'_i + \phi_0) \right] (t' - t'_i) - \frac{E_0 q}{\omega^2 m} [\cos(\omega t' + \phi_0) - \cos(\omega t'_i + \phi_0)], \quad (1)$$

where x_i and v_i are the corresponding position and velocity of particle at instant $t'_i = t'_n + T'$. Dissipation is not considered in this paper.

To describe the dynamics of the system, we obtain a mapping P that furnishes the velocity of the charged particle and phase of electric field at instants the particle leaves the region $x \in [0, d]$. We suppose that at the instant t'_n , the particle leaves the electric field region with velocity $\vec{v}(t'_n) = \vec{v}_n$. Then a magnetic field forces the particle to move in a circular trajectory with a constant angular velocity $\varpi = qH/m$. The particle describes a semicircle during the fixed time interval $T' = \pi m/Hq$. At the instant $t'_n + T'$, the particle is therefore re-injected into the electric field region with velocity $\vec{v}(t'_n + T') = -\vec{v}_n$. The field \vec{H} does not change the particle's energy. It works as a mechanism that injects the particle back to the field $\vec{E}(t')$. We assume the motion of the particle inside the electric field region occurs along a straight line. These considerations furnish good approximation in the limit of small d . We must say that the electromagnetic field

created due to the acceleration of the charged particle is disregarded in this paper.

Before we present the mapping, it is appropriate to define the following set of dimensionless variables:

$$\begin{aligned} t &= \omega t', & T &= \omega T' = \pi\tau, & \phi &= t + \phi_0 \\ X &= \frac{x}{d}, & \varepsilon &= \left(\frac{q}{m\omega^2 d} \right) E_0, \\ V &= \frac{v}{\omega d}, & \tau &= \left(\frac{\omega m}{q} \right) H^{-1}. \end{aligned} \quad (2)$$

For this set of dimensionless variables, the model presents only two relevant control parameters, namely ε and τ . For fixed values of d , ω , and the ratio q/m , the parameter ε denotes the dimensionless amplitude of oscillation of electric field, while τ represents the inverse of the dimensionless magnetic field.

It is important to mention that the returning time T to the region where electric field acts does not depend on the velocity of the particle, different from the FUM and FPM. In the FUM, the returning time is $T \propto 1/V$ therefore diverging in the limit of vanishing V . One can conclude that the phase of the moving wall, between collisions in the FUM and for small V , is highly uncorrelated therefore producing the chaotic sea. On the other hand, such a time is $T \propto V$ in the FPM producing uncorrelated phases upon collisions for the limit of large V . This loss of correlation leads the particle to experience Fermi acceleration.

In terms of the above variables, the two-dimensional mapping is written as

$$P : \begin{cases} V_{n+1} = -V_n + \varepsilon(\sin \phi_{n+1} - \sin(\phi_n + \pi\tau)) \\ \phi_{n+1} = \phi_n + \pi\tau + \Delta\mathcal{T}_{n+1} \bmod 2\pi, \end{cases} \quad (3)$$

where $\Delta\mathcal{T}_{n+1} = \omega\Delta T'_{n+1}$ is the interval of time at which the particle moves in the electric field. The term $\Delta\mathcal{T}_{n+1}$ corresponds to the smallest solution of $f(\Delta\mathcal{T}_{n+1}) = 0$, where $f(\Delta\mathcal{T}_{n+1})$ is

$$f(\Delta\mathcal{T}_{n+1}) = -D_{n+1} - [V_n + \varepsilon \sin(\phi_n + \pi\tau)]\Delta\mathcal{T}_{n+1} - \varepsilon[\cos\phi_{n+1} - \cos(\phi_n + \pi\tau)]. \quad (4)$$

The quantity $D_{n+1} = [X(t_{n+1}) - X(t_n + T)]$ represents the displacement of the particle with respect to the position at instants when it enters and leaves the region where the electric field is acting. When the particle moves from the right to left and crosses the electric field, we have $D_{n+1} = -1$. For the opposite situation, we have $D_{n+1} = 1$. Depending on the values of parameters and velocity, the particle enters and leaves the region where electric field acts at the same place, then $D_{n+1} = 0$. We used bisection method to solve Eq. (4) and an accuracy equals to 10^{-8} for the numerical solutions. A higher accuracy was tested, say 10^{-13} , and same results were obtained. Moreover, the simulations were carried out under double precision floating point representation.

The energy of the particle changes while it is immerse in the electric field. Such a field is the external excitation that introduces non-linearity to the motion of the particle. The parameter ε defines the strength of this non-linearity.

For $\varepsilon = 0$ we have $V_{n+1} = -V_n$ and, therefore, the system is integrable. For $\varepsilon \neq 0$, the dynamics is governed by a nonlinear term and the system experiences a transition from integrable to non-integrable regime. The phase space presents an intricate mixed structure containing periodic islands, chaotic parts characterized by positive Lyapunov exponents, and invariant KAM curves separating different portions of the phase space. Figure 2 shows the phase space of the system for different values of the control parameters ε and τ . The size of the chaotic seas is limited by KAM curves that prevent the particle to acquire unlimited energy gain. We see also that the variation of the control parameters affects both the position of the islands and the size of the chaotic region. Many other KAM curves exist beyond the smallest energy KAM curves. The phase space of the mapping preserves the following measure $d\mu = VdVd\phi$ given the determinant of the Jacobian matrix is $\det J = V_n/V_{n+1}$ (see Appendix for details).

The chaotic dynamics was characterized by the Lyapunov exponents. To guarantee a good convergence of the positive Lyapunov exponent, we defined an average λ that is written as

$$\lambda(\varepsilon, \tau) = \frac{1}{M} \sum_{j=1}^M \lambda_1(\phi_{0,j}, V_{0,j}),$$

where we considered an ensemble of $M = 10$ different initial conditions chosen in the chaotic sea and $\lambda_1(\phi_{0,j}, V_{0,j})$ is the positive Lyapunov exponent obtained for each initial condition $\phi = \phi_{0,j}$, $V = V_{0,j}$. Each initial condition was evolved $n = 10^8$ times. Figure 3(a) shows the average Lyapunov exponent as function of τ for $\varepsilon = 10^{-2}$, where the error bars represent the standard deviation calculated for the ensemble. For $\tau = 1$, the cyclotron frequency coincides with the frequency of the electric field. As a consequence, the trajectories

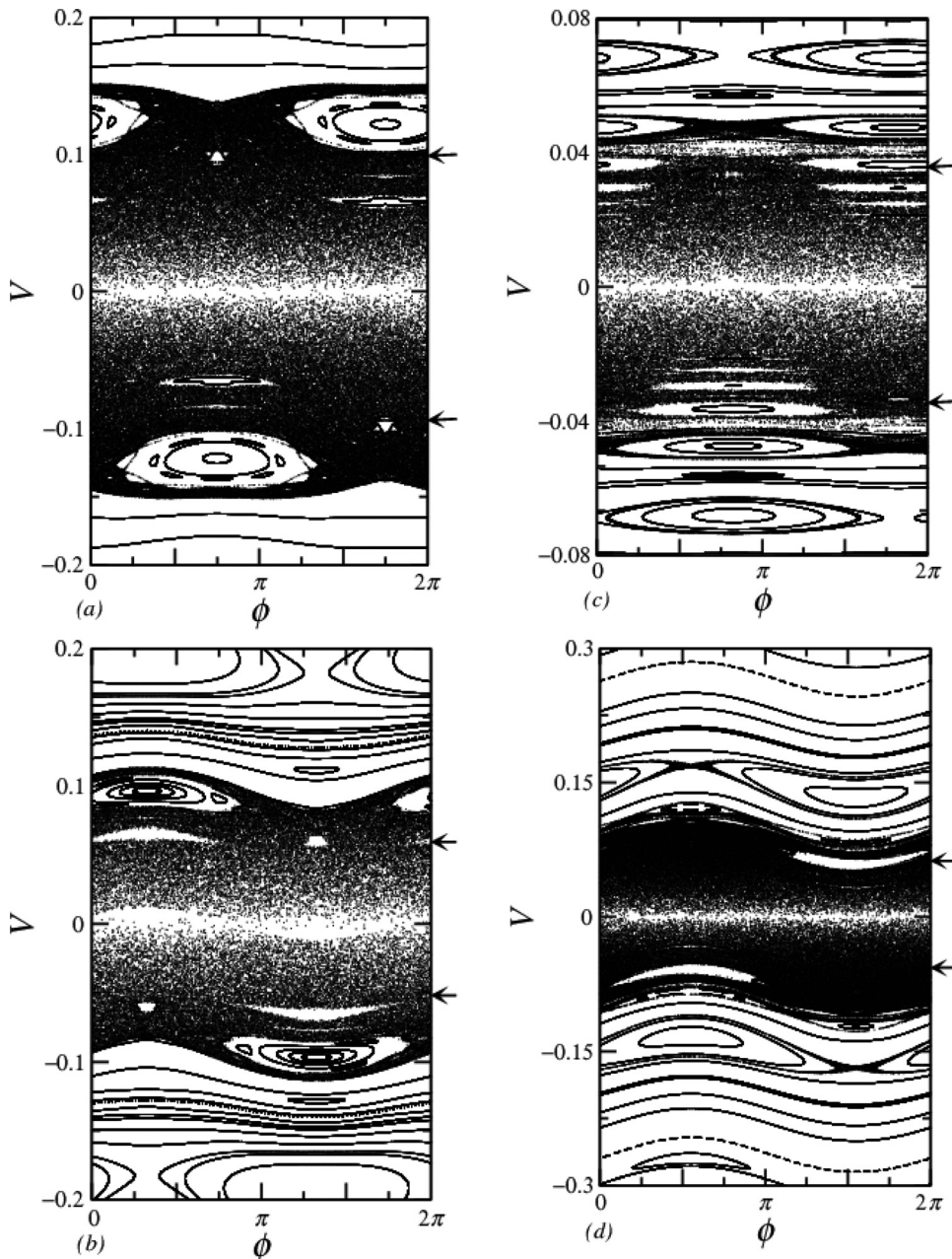


FIG. 2. These plots display the phase space of the system for different control parameters: (a) $\varepsilon = 10^{-2}$ and $\tau = 0.5$, (b) $\varepsilon = 10^{-2}$ and $\tau = 1.35$, (c) $\varepsilon = 10^{-3}$ and $\tau = 0.35$ and (d) $\varepsilon = 2 \times 10^{-2}$ and $\tau = 0.9$.

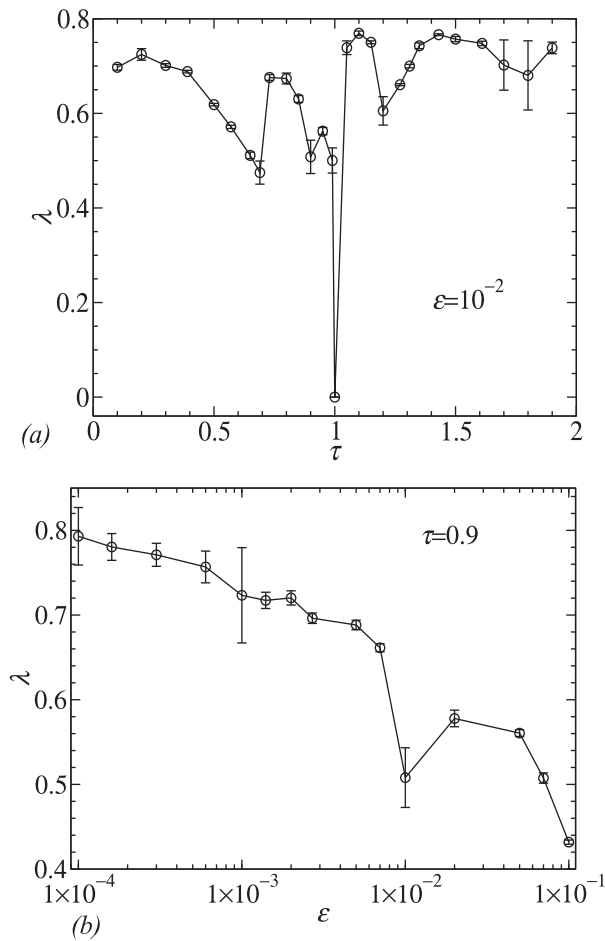


FIG. 3. These plots illustrate the average Lyapunov exponent as function of: (a) τ for constant $\varepsilon = 10^{-2}$ and; (b) as function of ε for fixed $\tau = 0.9$.

present a strong correlation with the electric field and no region of chaotic motion is observed. Such parameter configuration leads the Lyapunov exponent to assume null value. The same applies for τ equals to other odd values. For τ not odd, the trajectories lose correlation with the electric field yielding the particle to present chaotic motion. Similarly, for a fixed value of τ , the average Lyapunov exponent for different values of ε was also accounted, as shown in Fig. 3(b) for $\tau = 0.9$. We observe in Fig. 3(a) there is no apparent correlation between λ and τ . On the other hand, Fig. 3(b) shows that λ roughly decreases from $\lambda = 0.8$ till $\lambda = 0.4$, while the parameter ε increases a thousand times. Regarding the values of τ and ε in Fig. 3, the chaotic sea is characterized by the average Lyapunov exponent $\langle \lambda \rangle = 0.66 \pm 0.08$.

To illustrate the influence of the parameters ε and τ on the position of the lowest energy invariant KAM curve, we show in Figs. 4(a)–4(c) three different plots for the approximated location of the lowest invariant KAM curve for a set of three different ε considering different orders of magnitude. The size of the chaotic sea is relatively small when the parameter τ is near any odd value. The curves in Fig. 4 were constructed following the procedure: (i) We divided the ϕ range $[0, 2\pi)$ in 10^3 intervals of same size and we evaluated a single trajectory of an initial condition located at the chaotic sea. Such initial condition was iterated 10^9 times. (ii) We collected the greatest positive value of velocity and the smallest negative velocity for each ϕ interval. The plot of such data furnishes an approximated location of the lowest energy KAM curve.

We evaluated the average of the absolute value of velocity on the invariant KAM curves, namely V_{inv} , for different

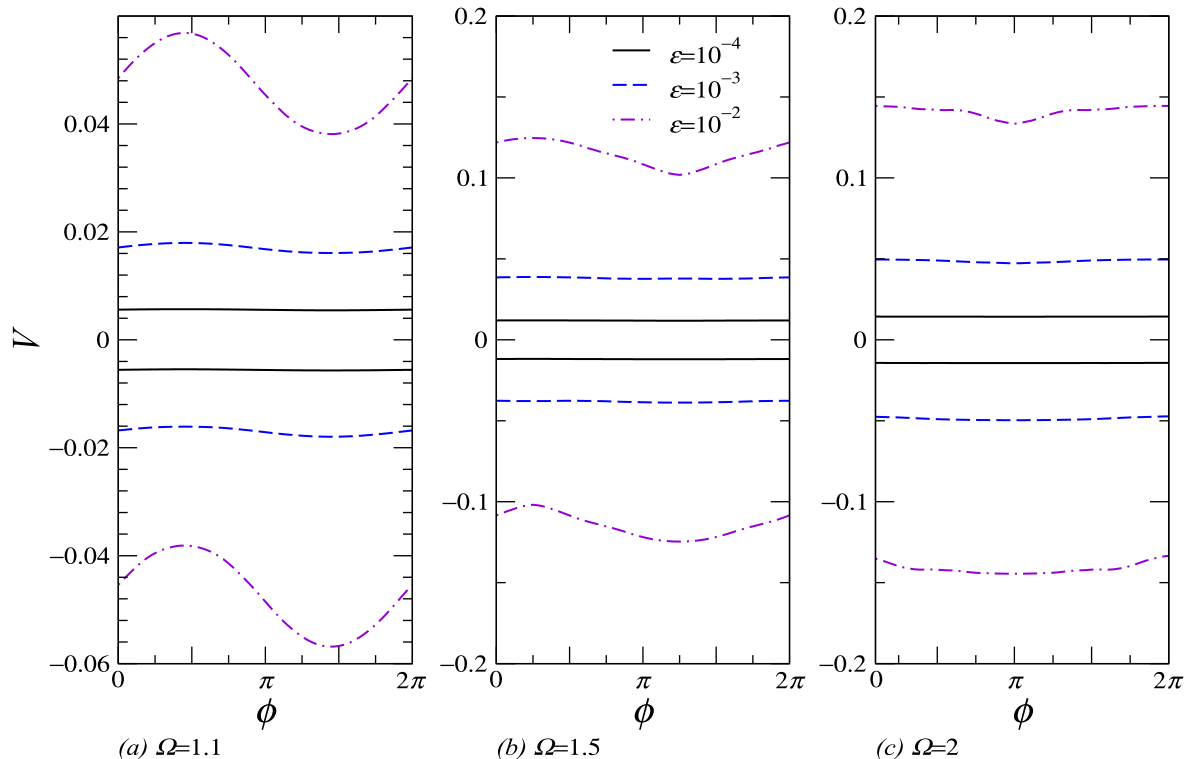


FIG. 4. This figure shows the position of the lowest energy invariant KAM curves for different values of ε and considering: (a) $\tau = 1.1$; (b) $\tau = 1.5$; and (c) $\tau = 2$.

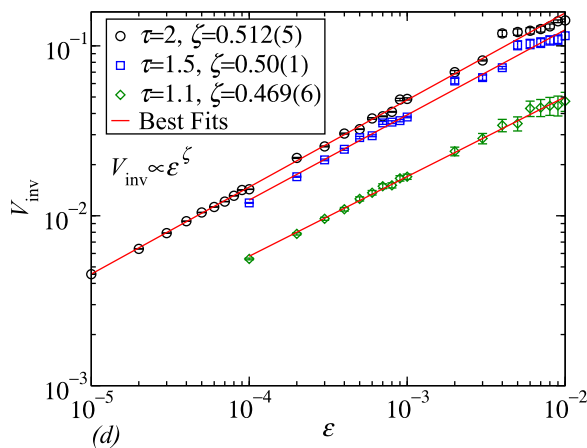


FIG. 5. The figure shows the average of the absolute values of the velocity of the KAM curves as function of ε for three different values of τ . The best fits furnish $V_{\text{inv}} \propto \varepsilon^\zeta$ with $\zeta \approx 0.5$.

combinations of parameters ε and τ . Figure 5 displays the results for $\tau = 1.1$, $\tau = 1.5$ and $\tau = 2$. We observe for all the situations that $V_{\text{inv}} \propto \varepsilon^\zeta$, with $\zeta \approx 0.5$.

III. SCALING PROPERTIES FOR THE TRANSPORT ON THE CHAOTIC SEA

Let us now concentrate more specifically on the transport properties through the chaotic sea limited by the KAM curves of lowest energy. To do so, we study the evolution of an ensemble of different initial conditions chosen at low velocity $V_0 = \varepsilon$ and with random phases $\phi_0 \in [0, 2\pi)$. We evolve each initial condition in time until it reaches a window of escape located inside the chaotic sea. We must stress however that there is no *real* escape of particles from the system. Indeed, the escape window is basically a specific position in the phase space where an ensemble of particles is let to evolve. When the escape happens, we collect the number of iterations spent and a new initial condition starts. We allow the particle to evolve up to a maximum of 10^9 iterations, if it does not escape before. Due to the stickiness and trapping near periodic regions, if a trajectory reaches the maximum iterations number, then a new initial condition starts. It is interesting to mention a historical paper of Karney²⁴ where stickiness was addressed. Indeed, he showed that depending on the control parameter, the correlation function may decay as a power law or as an exponential. After his historical paper, a galaxy of results was discussed for different types of systems. Results include anomalous chaotic transport for a Hamiltonian system with hyperbolic fixed points²⁵ and transport properties by the investigation of the first and second momenta for a standard-like map.²⁶

In our case, we define the escape window as the region of phase space located below the lowest energy KAM curve (LEKAMC) and above a value of velocity that we define as V_{esc} . We define the value of V_{esc} in terms of the LEKAMC as $V_{\text{esc}} = g V_s$, where V_s denotes the absolute value of lowest velocity along the LEKAMC and g is a constant. For this paper, we use $g = 0.7$, although other values can also be chosen. As discussed in Ref. 29, the value of the escape velocity influences the time the particle spends until it reaches such a

value but the universal features are unaltered with respect to g . The arrows on right side of each phase space of Fig. 2 represent the values V_{esc} for those values of parameters. Given we want to consider large portions of chaotic components to study transport along such region, from now on we fix $\tau = 2$ and describe some properties as functions of n and ε .

Evolving the simulation over an ensemble of M different initial conditions, we obtain the number $H(n)$ of orbits that satisfies the condition $|V_n| > V_{\text{esc}}$ at each iteration number n . This quantity depends on the size of the ensemble. To avoid such a dependence, we regard the normalized observable

$$h(n) = \frac{H(n)}{M}.$$

This quantity is the escape distribution of particles. The observable $h(n)$ fluctuates largely for small size of the ensemble. So we used ensembles of $M = 10^7$ different initial conditions. Figure 6(a) shows a plot of $h(n)$ vs. n for different values of ε .

We observe that each curve of h exhibit an initial growth regime reaching a maximum value h_{max} . After that, it decreases approaching zero asymptotically. We define n_x as the value of n where $h \approx h_{\text{max}}$. It is clear from the figure that the smaller the parameter ε , the greater n_x . An immediate consequence is that when ε decreases, the longer the simulation.

To obtain an accurate value of n_x , we consider that the portion near the peak of the curve $h(n)$ is locally described by a quadratic function. The coefficients of such a curve are

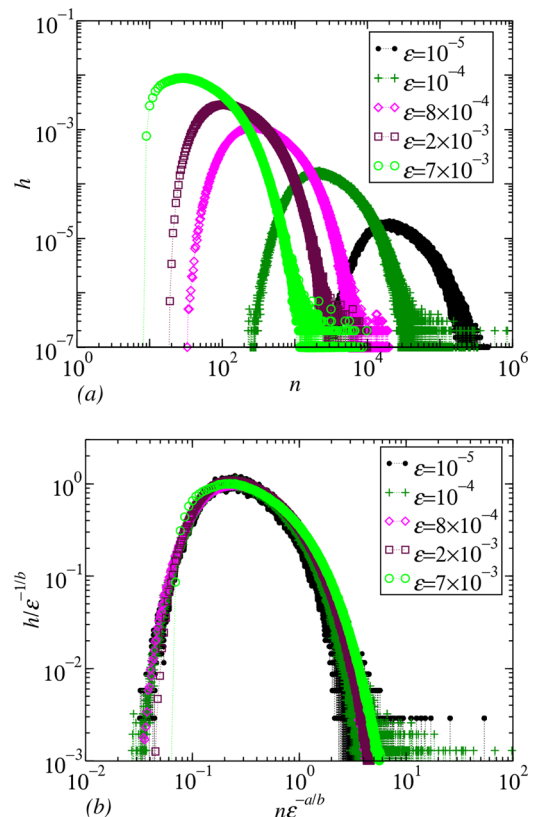


FIG. 6. (a) shows the plot of the normalized number of escaping orbits at the iteration n for different values of ε and fixed $\tau = 2$. (b) displays the overlap of all curves shown in (a) onto a single plot, after a suitable rescaling of the axis.

obtained by a quadratic fit. Moreover, the maximum is easily obtained by setting the derivative to zero; this gives a good approximation for n_x . Figure 7(a) shows a plot of n_x vs ε . The best fit to the numerical data furnishes $n_x \propto \varepsilon^z$ with $z = -0.98 \pm 0.02$. This result is in remarkably well agreement with those obtained for a periodically corrugated waveguide.³⁰ We obtained also the corresponding value of h_{\max} for each curve of Fig. 6(a), as it is displayed in Fig. 7(b). We suppose that $h_{\max} \propto \varepsilon^\gamma$ where a fitting gives $\gamma = 0.95 \pm 0.05$.

From the results shown in Figs. 7(a) and 7(b), we suppose that the quantity h can be formally described in terms of a scaling relation of the type

$$h(n, \varepsilon) = lh(l^a n, l^b \varepsilon), \quad (5)$$

where l is a scaling factor, a and b are scaling exponents. For $l = \varepsilon^{-1/b}$, the above equation becomes

$$h(n, \varepsilon) = \varepsilon^{-1/b} f(\varepsilon^{-a/b} n), \quad (6)$$

where $f(\varepsilon^{-a/b} n) = h(\varepsilon^{-a/b} n, 1)$. For $n \approx n_x$, near $h = h_{\max}$, the above expression furnishes

$$n_x \propto \varepsilon^{a/b}.$$

Moreover,

$$h(n_x, \varepsilon) \propto \varepsilon^{-1/b}.$$

Considering the two different expressions for the scaling factors, we have that $z = a/b$ and $\gamma = -1/b$. Therefore, we

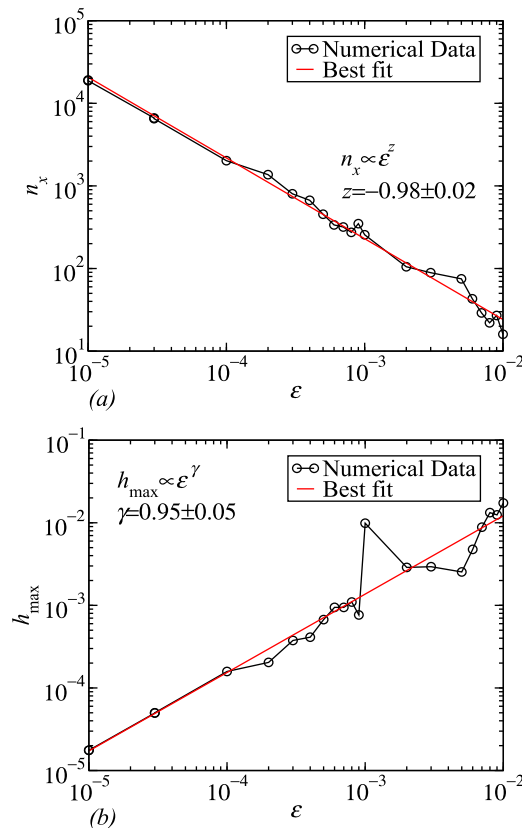


FIG. 7. (a) illustrates the crossover n_x as function of ε . The best fit furnishes $n_x \propto \varepsilon^z$ with $z = -0.98 \pm 0.02$. (b) illustrates the maximum values of h as function of ε . The best fit furnishes $h_{\max} \propto \varepsilon^\gamma$ with $\gamma = 0.95 \pm 0.05$.

obtain $a = -z/\gamma = 1.03 \pm 0.06$ and $b = -1.05 \pm 0.06$. When these exponents are conveniently applied to rescale the axes of Fig. 6(a), all curves are overlapped onto a single plot, as shown in Fig. 6(b).

As far we discussed the results for escaping orbits, let us now concentrate to describe the behavior of the orbits that survive longer (do not escape) as function of n . We define

$$\eta_{\text{surv}}(n) = \frac{N_{\text{surv}}}{M},$$

where the quantity η_{surv} represents the normalized number of orbits that do not escape until time n . Figure 8(a) shows a plot of η_{surv} vs. n for different values of parameter ε . As it is expected, η_{surv} is essentially one for small n and it decreases for increasing n .

We observe that η_{surv} presents two different decay regimes, as illustrated in Fig. 8(b). In the initial regime, η_{surv} decays exponentially, i.e., $\eta_{\text{surv}} = c_1 \exp(\beta_1 n)$, where c_1 is a constant and β_1 is an exponent. For large enough n , the curves of η_{surv} decay according to a power law of type $\eta_{\text{surv}} = c_2 n^{\beta_2}$, where c_2 is a constant and β_2 is an exponent. The inset in Figure 8(b) shows, in a log-linear plot, the details of the initial decay regime and the crossover when the exponential decay becomes a power law decay. As discussed in Ref. 21, the exponential decay is mostly observed when a particle is moving along a chaotic region where no periodic islands are observed. In our model, this chaotic component corresponds to the region below the islands and exponential decay dominates over the survival orbits. However, when the particle is

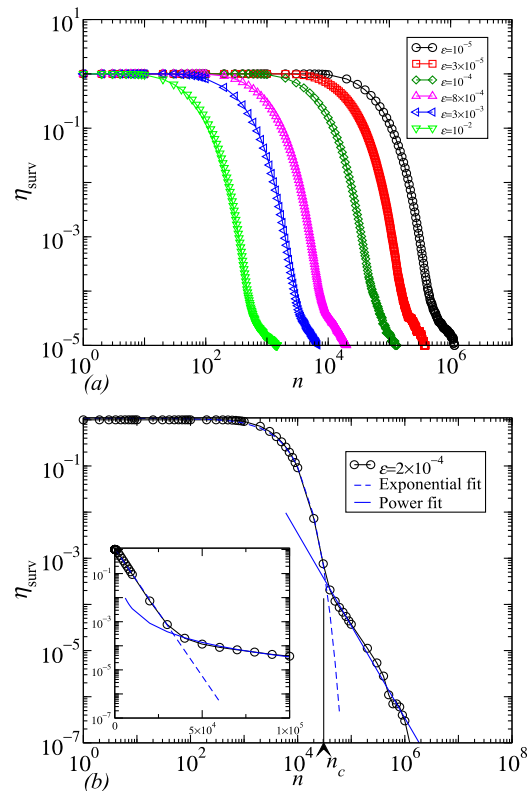


FIG. 8. (a) displays the normalized number of remaining orbits (do not escape) as function of n and different values of ε ; (b) illustrates the decay of the quantity η_{surv} showing evidently two regimes.

increasing energy, the periodic islands start to be visible by the particle leading, therefore, to trapping and consequently to stickiness. This dynamical regime, as discussed in Ref. 22, produces a decay characterized by a power law type. We observe a changeover from one kind of decay to another one as the velocity of the particle increases. For each curve of η_{surv} , there is a value $n = n_c$ characterizing the changeover from exponential to power law decay. Fitting the two decays property, we obtain the coefficients c_1 , c_2 , β_1 and β_2 for each η_{surv} curve. We find the values n_c for each value of ε and the best fit to the numerical data furnishes $n_c \propto \varepsilon^\alpha$ with $\alpha = -0.92 \pm 0.05$, as shown in Fig. 9(a). It is important to mention that this type of behavior for the survival probability was already observed before. Indeed, for some Hamiltonian systems, the escape is described by a survival probability of exponential type for short time and a power law for long enough time.²⁷ Similar behavior was also observed for the recurrence time, where an exponential decay and a power law decay coexist.²⁸

In our approach, this behavior changing from exponential to power law decay can also be described via the scaling formalism, as we have made before. The exponent obtained from the crossover plot in Fig. 9(a) allows us to rescale conveniently the axis and overlap the curves of survival probability shown in Fig. 8(a) onto a single plot as shown in Fig. 9(b). This result gives strong evidences that the survival probability is scaling invariant with respect to the parameter ε .

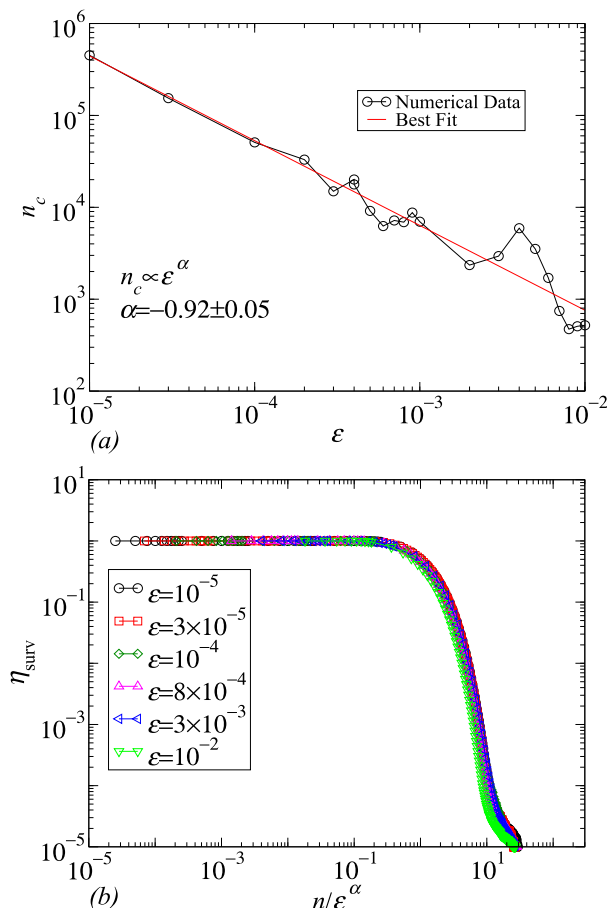


FIG. 9. (a) shows the numerical data of crossover of η_{surv} . The best fit furnishes $n_c \propto \varepsilon^\alpha$ with $\alpha = -0.92 \pm 0.05$. Appropriate scaling transformation overlaps the η_{surv} curves onto a single plot, as displayed in (b).

Recent results discussed for a time-dependent potential well²⁹ considered the dynamics as a function of three effective control parameters. In our case, keeping fixed the parameter τ , we have only the liberty to consider variation of the control parameter ε . Therefore, for short n and low energy, if the transport of particles along the chaotic sea was similar to the so called normal Brownian diffusion, the number of entrances of the particles in the region of the active electric field required to diffuse on average until an escaping velocity had to be proportional to V_{esc}^2 . However, the dynamical exponents of both n_x and n_c are $z \cong \alpha \cong -1$. We observe in Figs. 7(a) and 9(a) that n_c is roughly thirty times greater than n_x for each value of ε . This result means that h_{max} occurs before the transition from exponential to power law decay of surviving probability η_{surv} . As discussed before, $V_{\text{inv}} \propto \varepsilon^\zeta$, $\zeta \approx 1/2$ (Fig. 5). As V_{esc} is a fraction of invariant KAM curve, it is natural to write $V_{\text{esc}} \propto \varepsilon^{1/2}$. Moreover, we obtained $h_{\text{max}} \propto \varepsilon^\gamma$, $\gamma \approx 1$ (Figure 7(b)). These expressions furnish $h_{\text{max}} \propto V_{\text{esc}}^2$ and $n_x \propto V_{\text{esc}}^{-2}$. Thus, we have that the trajectories in the chaotic sea do not evolve as a normal Brownian diffusion. There are regions at low energy of phase space where very small islands of regular motion leads the trajectories to experience stickiness from time to time.²⁹ It was recently studied as an application of a double well potential in chemistry regarding the survival probability and the escape process from one well to the other one due to noise.³¹ Indeed, the survival probability was shown to be exponential when the escape from one well to the other one is quick while long trapping leads the survival probability to change from exponential to a power law. For the results,²⁹ considering large n , depending on the control parameters, the decay curve can exhibit more complicate regimes including stretched exponential.²³ For the range of control parameters considered in the present paper, and for the interval of simulation, the stretched exponential behavior was not observed.

Let us now discuss the results obtained for this paper. The mixed structure observed in the phase space led us to obtain a positive Lyapunov exponent for the chaotic sea. The size of the chaotic sea is dependent on the control parameters and it scales with the nonlinear parameter ε as $\varepsilon^{1/2}$ for the values of control parameter τ used in the paper. The chaotic sea appears coexisting with periodic islands. If the escaping hole is placed below the periodic islands, the survival probability is observed to be exponential, according to the results present in the literature.^{25,26,28} The survival probability was also shown to decay exponentially in the Henon-Heiles potential for high energy rising the predictability of the system.³² On the other hand, when the position of the hole is moved in the phase space in such a way that periodic islands exist, the orbits have the chance of getting trapped during the dynamics. The temporary trapping leads to anomalous diffusion²⁵ and the survival probability suffers a changeover to a slower decay. Indeed, in our results, we observe a change to power law decay. Several results observed in the literature also noticed this changeover.^{28,31} A universality was proposed recently for the recurrence time²⁷ and power law decay was observed in different regions of the phase space for 2-D Hamiltonian systems³³⁻³⁶ and for higher degrees of freedom Hamiltonian systems.³⁷

As a further work, we plan to investigate the dynamics of the system in the transition from regular to chaotic trajectories, observed near odd values of the parameter τ . It is also our plan to consider the dynamics under the presence of dissipation due to the motion of the particle in a viscous fluid. When such a dissipation acts on the particle attractors are observed in phase space.

IV. CONCLUSIONS

We studied some dynamical properties for an ensemble of non-interacting particles in an accelerator of charged particles. In terms of dimensionless variables, the system presents two control parameters: (i) ε that is related to the amplitude of oscillation of the electric field and; (ii) τ associated to the magnetic field. The parameter ε defines the strength of the non-linearity and the parameter τ defines the re-injection time of particle in the electric field. When τ assumes odd values, the trajectories in phase space present strong correlation with the oscillating electric field and, therefore, chaotic regions are not observed. Such a correlation does not occur for non odd values of τ and the phase space presents chaotic trajectories coexisting with regions of regular motion and invariant KAM curves. The transition from regular to chaotic orbits near odd values of τ is difficult to be characterized mainly due to the relative small size of chaotic sea in this transition.

We proposed a homogeneous function leading to the scaling exponents that describe the escape and transport of particles through the chaotic sea. We used this scaling description to overlap all the curves of the escape distribution onto a single plot.

The survival probability, which characterizes the dynamics of the orbits that last longer in the dynamics until reach the escape limit, presents two decay regimes. For short values of n , the quantity η_{surv} decays exponentially while it is a power law for large n , marking clearly the existence of sticky orbits in phase space. Appropriate scaling transformations overlap all curves of η_{surv} onto a single plot.

ACKNOWLEDGMENTS

D.G.L. thanks to FAPEMIG, CNPq, and FAPESP. E.D.L. thanks to FAPESP, CNPq, and FUNDUNESP, Brazilian agencies. The authors acknowledge Carl P. Dettmann for a careful reading of the paper. This research was supported by resources supplied by the Center for Scientific Computing (NCC/GridUNESP) of the São Paulo State University (UNESP).

APPENDIX: JACOBIAN MATRIX COEFFICIENTS

The coefficients of the Jacobian matrix are given by

$$J = \begin{pmatrix} \frac{\partial V_{n+1}}{\partial V_n} & \frac{\partial V_{n+1}}{\partial \phi_n} \\ \frac{\partial \phi_{n+1}}{\partial V_n} & \frac{\partial \phi_{n+1}}{\partial \phi_n} \end{pmatrix},$$

where

$$\frac{\partial V_{n+1}}{\partial V_n} = \frac{-V_{n+1} + \varepsilon \cos \phi_{n+1} \Delta \mathcal{T}_{n+1}}{V_{n+1}},$$

$$\frac{\partial V_{n+1}}{\partial \phi_n} = \frac{\varepsilon}{V_{n+1}} \{ [-V_n + \varepsilon \cos(\phi_n + \pi\tau) \Delta \mathcal{T}_{n+1}] \cos \phi_{n+1} - V_{n+1} \cos(\phi_n + \pi\tau) \},$$

$$\frac{\partial \phi_{n+1}}{\partial V_n} = \frac{\Delta \mathcal{T}_{n+1}}{V_{n+1}},$$

$$\frac{\partial \phi_{n+1}}{\partial \phi_n} = \frac{-V_n + \varepsilon \cos(\phi_n + \pi\tau) \Delta \mathcal{T}_{n+1}}{V_{n+1}}.$$

¹E. Fermi, *Phys. Rev.* **75**, 1169 (1949).

²A. V. Milovanov and L. M. Zelenyi, *Phys. Rev. E* **64**, 052101 (2001).

³A. Veltri and V. Carbone, *Phys. Rev. Lett.* **92**, 143901 (2004).

⁴K. Kobayakawa, Y. S. Honda, and T. Samura, *Phys. Rev. D* **66**, 083004 (2002).

⁵G. Lanzano *et al.*, *Phys. Rev. Lett.* **83**, 4518 (1999).

⁶F. Saif, I. Bialynicki-Birula, M. Fortunato, and W. P. Schleich, *Phys. Rev. A* **58**, 4779 (1998).

⁷A. Steane, P. Szriftgiser, P. Desbiolles, and J. Dalibard, *Phys. Rev. Lett.* **74**, 4972 (1995).

⁸A. Loskutov and A. B. Ryabov, *J. Stat. Phys.* **108**, 995 (2002).

⁹A. J. Lichtenberg and M. A. Lieberman, *Regular and Chaotic Dynamics*, Applied Mathematical Science Vol. 38 (Springer-Verlag, New York, 1992).

¹⁰M. A. Lieberman and A. J. Lichtenberg, *Phys. Rev. A* **5**, 1852 (1972).

¹¹L. D. Pustilnikov, *Trudy Moskow Mat. Obshch.* **34**(2), 1 (1977); *Theor. Math. Phys.* **57**, 1035 (1983); *Sov. Math. Dokl.* **35**(1), 88 (1987); *Russ. Acad. Sci. Sb. Math.* **82**(1), 231 (1995).

¹²A. J. Lichtenberg, M. A. Lieberman, and R. H. Cohen, *Physica D* **1**, 291 (1980).

¹³E. D. Leonel and P. V. E. McClintock, *J. Phys. A* **38**, 823 (2005).

¹⁴D. G. Ladeira and E. D. Leonel, *Chaos* **17**, 013119 (2007).

¹⁵J. D. Meiss, *Rev. Mod. Phys.* **64**, 795 (1992).

¹⁶H. Thisgaard, D. R. Elema, and M. Jensen, *Med. Phys.* **38**, 4535–4541 (2011).

¹⁷H. Thisgaard, M. Jensen, and D. R. Elema, *Appl. Radiat. Isot.* **69**, 1–7 (2011).

¹⁸W. Kleeven, M. Abs, J. L. Delvaux *et al.*, *Nucl. Instrum. Methods Phys. Res. B* **269**, 2857–2862 (2011).

¹⁹N. Puttaraksa, S. Gorelick, T. Sajavaara *et al.*, *J. Vac. Sci. Technol. B* **26**, 1732–1739 (2008).

²⁰S. Gorelick, N. Puttaraksa, T. Sajavaara *et al.*, *Nucl. Instrum. Methods Phys. Res. B* **266**, 2461–2465 (2008).

²¹E. G. Altmann, A. E. Motter, and H. Kantz, *Phys. Rev. E* **73**, 026207 (2006).

²²E. G. Altmann, E. C. da Silva, and I. L. Caldas, *Chaos* **14**, 975 (2004).

²³C. P. Dettmann and E. D. Leonel, *Physica D* **241**, 403 (2012).

²⁴C. F. F. Karney, *Physica D* **8**, 360 (1983).

²⁵S. S. Abdullaev and K. H. Spatschek, *Phys. Rev. E* **60**, R6287 (1999).

²⁶L. Cavallasca, R. Artuso, and G. Casati, *Phys. Rev. E* **75**, 066213 (2007).

²⁷H. E. Kandrup *et al.*, *Chaos* **9**, 381 (1999).

²⁸N. Buric, A. Rampioni, G. Turchetti, and S. Vaienti, *J. Phys. A: Math. Gen.* **36**, L209 (2003).

²⁹D. R. da Costa, C. P. Dettmann, and E. D. Leonel, *Phys. Rev. E* **83**, 066211 (2011).

³⁰E. D. Leonel, D. R. da Costa, and C. P. Dettmann, *Phys. Lett. A* **376**, 421 (2012).

³¹B. Dybiec, *J. Chem. Phys.* **133**, 244114 (2010).

³²F. Blesa *et al.*, *Int. J. Bifurcation Chaos* **22**, 1230010 (2012).

³³V. A. Avetisov and S. K. Nechaev, *Phys. Rev. E* **81**, 046211 (2010).

³⁴R. Venegeroles, *Phys. Rev. Lett.* **101**, 054102 (2008).

³⁵R. Venegeroles, *Phys. Rev. Lett.* **102**, 064101 (2009).

³⁶G. Cristadoro and R. Ketzmerick, *Phys. Rev. Lett.* **100**, 184101 (2008).

³⁷D. L. Shepelyansky, *Phys. Rev. E* **82**, 055202(R) (2010).